W360–W367 *Nucleic Acids Research, 2010, Vol. 38, Web Server issue* *Published online 11 May 2010*
doi:10.1093/nar/gkq371

SIREs: searching for iron-responsive elements

Monica Campillos[1], Ildefonso Cases[2], Matthias W. Hentze[1] and Mayka Sanchez[1,2,*]

[1]European Molecular Biology Laboratory (EMBL), Meyerhofstrasse 1, 69117 Heidelberg, Germany and [2]Institute of Predictive and Personalized Medicine of Cancer (IMPPC), Crta Can Ruti, Camí de les Escoles s/n, 08916 Badalona, Barcelona, Spain

Received January 23, 2010; Revised April 21, 2010; Accepted April 26, 2010

ABSTRACT

The iron regulatory protein/iron-responsive element regulatory system plays a crucial role in the post-transcriptional regulation of gene expression and its disruption results in human disease. IREs are *cis*-acting regulatory motifs present in mRNAs that encode proteins involved in iron metabolism. They function as binding sites for two related *trans*-acting factors, namely the IRP-1 and -2. Among *cis*-acting RNA regulatory elements, the IRE is one of the best characterized. It is defined by a combination of RNA sequence and structure. However, currently available programs to predict IREs do not show a satisfactory level of sensitivity and fail to detect some of the functional IREs. Here, we report an improved software for the prediction of IREs implemented as a user-friendly web server tool. The SIREs web server uses a simple data input interface and provides structure analysis, predicted RNA folds, folding energy data and an overall quality flag based on properties of well characterized IREs. Results are reported in a tabular format and as a schematic visual representation that highlights important features of the IRE. The SIREs (Search for iron-responsive elements) web server is freely available on the web at http://ccbg.imppc.org/sires/index.html

INTRODUCTION

Post-transcriptional gene regulation including mRNA stability regulation and translational control is an integral part of gene expression and enables more rapid responses and fine-tuning of cell changing conditions (1). The coordinated expression of cellular iron homeostasis by the iron regulatory protein/iron-responsive element regulatory system is among the best characterized post-transcriptional regulatory mechanisms in vertebrates (2). This system involves two cytoplasmic iron regulatory proteins, IRP1 and IRP2, and RNA stem–loop, known as IREs, within transcripts encoding iron metabolism proteins. Under conditions of iron starvation, IRPs bind to the IREs and control the expression of target mRNAs by two different mechanisms. Either of the IRPs induces translational repression when bound to an IRE located at the 5′ UTR, whereas their association with IREs in the 3′ UTR mediates mRNA stabilization (3,4). The central role of the IRPs in iron homeostasis is highlighted by the observation that total and constitutive genetic ablation of both IRP1 and IRP2 causes embryonic lethality in mice (5). Furthermore, tissue-specific disruption of both IRPs in duodenal enterocytes revealed that these proteins are essential for intestinal function (6).

IREs have been reported in a total of 12 mRNAs, 7 containing an IRE in their 5′ UTRs and 5 in their 3′ UTRs. 5′ UTR IREs include those present in the mRNAs coding for the iron storage proteins ferritin L (FTL) and ferritin H (FTH1; 7), the heme biosynthesis enzyme ALAS2 (8), the iron exporter ferroportin (SLC40A1; 9), two enzymes of the citric acid cycle (mitochondrial aconitase ACO2 and *Drosophila melanogaster* succinate dehydrogenase dSDH; 10) and the transcription factor and oxygen sensor EPAS1 (also known as HIF2alpha; 11). 3′ UTR IREs have been identified in mRNAs for iron acquisition molecules (TFR1 and SLC11A2; 12,13), the human cell-cycle phosphatase CDC14A (14), the human myotonic dystrophy kinase-related Cdc42-binding kinase alpha (CDC42BPA; 15) and the mouse glycolate oxidase (Hao1; 16). In humans, the failure to coordinate the expression of IRE-containing genes is associated with pathologic conditions, as illustrated by the autosomal dominant hyperferritinemia-cataract syndrome observed in patients carrying mutations in the FTL IRE (17; HHCS, OMIM 600886), or by an autosomal dominant iron overload syndrome associated with a mutation in the FTH1 IRE (18; OMIM 134770).

A canonical IRE structure is composed of a 6-nt apical loop (5′-CAGWGH-3′; whereby W stands for A or U and

*To whom correspondence should be addressed. Tel: 0034935543077; Fax: 0034934651472; Email: msanchez@imppc.org

The authors wish it to be known that, in their opinion, the first two authors should be regarded as joint First Authors.

H for A, C or U) on a stem of five paired nucleotides, a small asymmetrical bulge with an unpaired cytosine on the 5′ strand of the stem, and an additional lower stem of variable length. The first (C14) and the fifth (G18) nucleotides of the terminal loop pair, forming an AGW pseudo-triloop and leaving position 19 unpaired (19,20). *In vitro* selection procedures have yielded several IRE-like structures with alternative nucleotide composition in the apical loop, yet able to bind IRP1 and/or IRP2 (21–23). In addition, several IREs present a non-canonical structure with an unpaired bulge nucleotide on the 3′ strand of the upper stem (i.e. IRE of SLC11A2 and EPAS1) or a mismatch pair in the upper stem (i.e. IRE of Hao1). These data indicate that the primary and secondary structure of an IRP-binding IRE-like motif is more variable and flexible than had previously been recognized. Indeed, current available programs (i.e. RNAAnalyzer, UTRScan and RNAMotif; 24–26) to predict IREs do not show a satisfactory level of sensitivity and fail to detect functional non-canonical IREs identified by our group and others (11,13). To overcome this limitation, we have created a new software tool dedicated to predict IREs and implemented as a web server tool easy to use for the entire research community.

MATERIALS AND METHODS

IRE prediction algorithm

The SIREs algorithm is implemented on a Perl script that screens for a 19 or 20 nucleotide sequence motif corresponding to the core sequence of an IRE (positions n07–n25) that includes the hexa-apical hairpin loop (n14–n19), the upper stem, the cytosine bulge (C8) and the lower base pair (n07–n25) (Figure 1A). This core IRE region is sufficient to establish the recently reported RNA binding hierarchy between IRP1 and 5′ IREs (27). We used a highly specific rule-based decision tree shown in Figure 1B to screen for IRE motifs in nucleotide sequences. First, the sequences are screened to find one of the motifs described in Figure 1 (motif 1–18). These 18 motifs are based on two canonical IRE motifs 5′-CNNNNNCAGUGN-3′ (motif 1) and 5′-CNNNNNCAGAGN-3′ (motif 2) and 16 SELEX (systematic evolution of ligands by exponential enrichment) motifs proven to bind IRP1 and/or IRP2 *in vitro* with a relative binding efficiency >20% (21–23). All motifs but motif 18 contain a cytosine at position n8; motif 18 has a guanine. Next, pairing of the upper stem nucleotides is tested allowing six pairing combinations (four Watson–Crick base pairs: A–U, U–A, C–G, G–C, and two wobble base pairs: U.G and G.U). The number of G.U or U.G wobble base pairs in the upper stem and at position n07–n25 is limited to a maximum of two, since the presence of three or more wobble base pairs impairs the formation of a proper IRE (data not shown). The SIREs program allows the detection of IRE-like motifs with one mismatch in the upper stem (positions n13–n20, n12–n21, n11–n22, n10–n23, n09–n24) or at position n07–n25, in order to detect IREs like the one present in the Hao1 mRNA, which contains an A:A mismatch at position n11–n22. Similarly, a single bulge in the 3′ half of the upper stem (3′ bulge) is allowed at positions n20b, n21b, n22b or n23b to detect IREs such as the ones present in the mRNA of SLC11A2 or EPAS1 (U bulge position n21b). The acceptance of one 3′ bulge nucleotide or one mismatch in the upper stem or at position n07–n25 is mutually exclusive. Once a sequence fulfilling all these criteria has been identified, six additional nucleotides of the lower stem are obtained and reported. Predicted folding free energy (RNAfold program, Vienna package) is also reported by SIREs program and considered in the quality scoring system (see below).

Web server

The SIREs web server program uses a simple input that allows easy handling and provides output reports with detailed information for prediction of IREs. The server can accept single or multiple DNA or RNA sequence entries in FASTA format. For performance reasons, there is a limit of 500 000 residues to be submitted. The server takes between 15 and 60 s for handling such input.

A partial sequence of the 5′ UTR of the mouse ferritin-H cDNA (GenBank Accession number: NM_010239, nucleotides 1–240) that contains an IRE is used as a rapid testing example (Figure 2). In addition, a pre-compiled result page using a multi-sequence query input is also provided as a more complex example. Extensive documentation on the algorithm, the server and the biological system is provided in the documentation, FAQs and references sections; there is also a straightforward way to contact the team to make suggestions and to report problems (Figure 2).

The output includes the total number of submitted sequences and predicted IREs, and it is stored at specific addresses, which can be bookmarked for later retrieval or inspection. Results are reported in tabular format (Figure 3B) for rapid inspection as well as by a schematic visual representation (Figure 3B and C) that highlights important features of the IRE motif in colors (i.e. apical loop in red, C8 bulge in green, G.U or U.G wobble base pairs in orange, 3′ bulge or upper stem mismatch in yellow). Both tabular and visual data are hyperlinked to each other. The tabulated list can be sorted by several criteria including mapped IRE start and end positions, loop type, free energy and quality flag and its content can be downloaded in GFF format (general feature format, see http://song.sourceforge.net/gff3.shtml for full description of GFF), which allows rapid machine processing. The sequence surrounding the predicted IRE (sequence context) is shown with the primary IRE sequence in red, which can be downloaded in FASTA format for further analysis (i.e. BLAST search of conserved IRE in orthologous genes; Figure 3D).

A SIREs prediction reports information on the nucleotide composition of the apical loop (canonical motifs: 1 and 2 or SELEX motifs: 3–18) and the presence of: one mismatch base pair or one 3′ bulged nucleotide in the upper stem, a guanine (G) at position n25, and the number of wobble base pairs. The presence of the nitrogenous base guanine at position n25 should be taken with

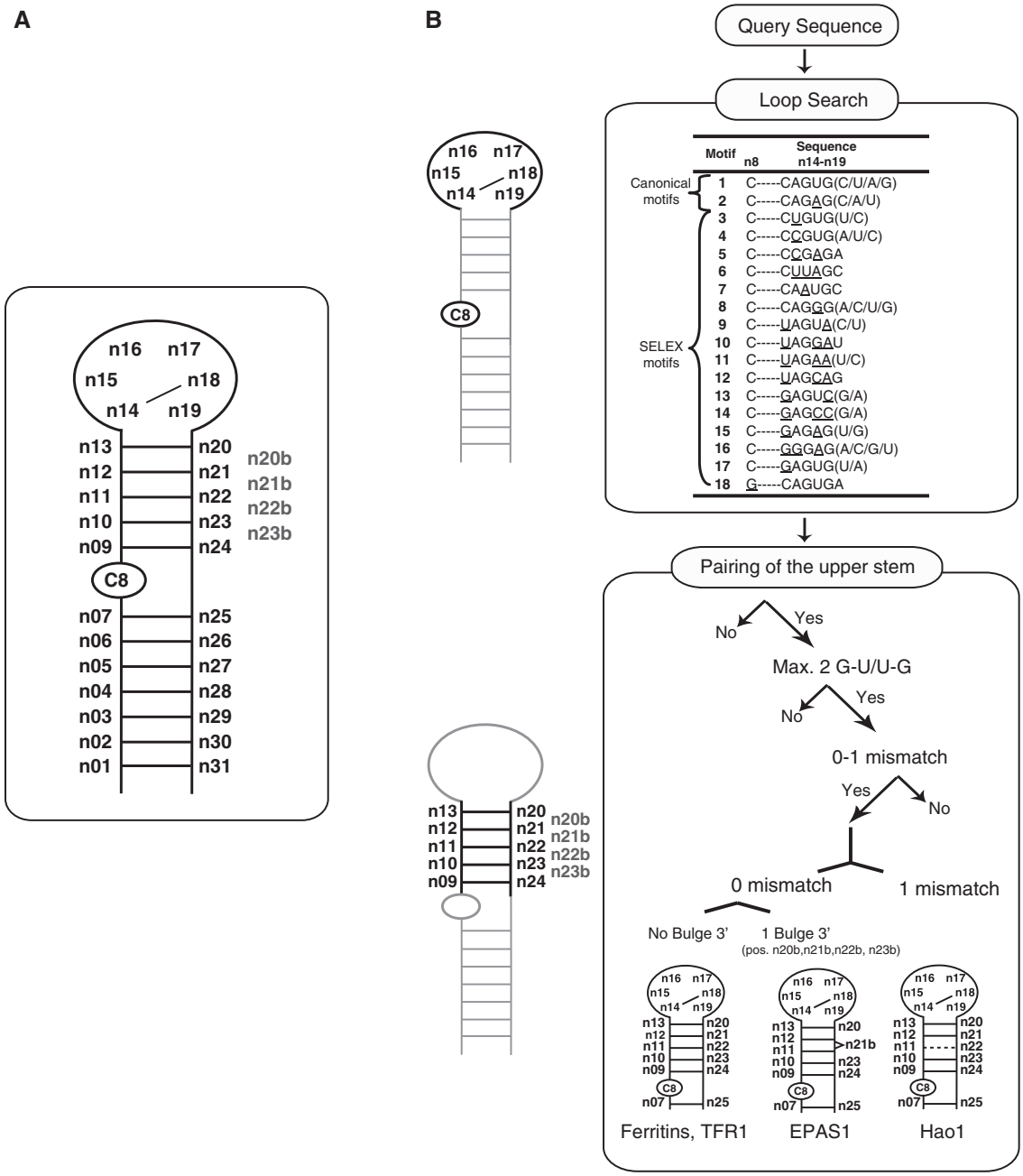

Figure 1. (**A**) Schematic representation of an IRE. The SIREs prediction program allows the detection of IREs with 18 different apical motifs, one bulge at the 3′ (n20b, n21b, n22b and n23b) or one mismatch in the upper stem. (**B**) Main workflow of the SIREs prediction algorithm. Prediction is limited to the core IRE sequence containing the hexa-apical loop (n14–n19), the C8 bulge, the upper stem and the base pair n07–n25. After finding a matching sequence, additional nucleotides from the lower stem are also obtained and reported (n01–n06 and n26–n31).

caution since it may pair with the cytosine (C8) bulge and could hence impair the formation of a proper IRE. These features are taken into account for the acquisition of an overall quality IRE prediction flag.

In addition to the SIREs predicted structure (Figure 3B), the putative IRE is folded using the RNAfold program from the Vienna RNA package (28), a well-established compendium of tools for the prediction and comparison of RNA secondary structures (Figure 3C). Both graphical representations can be exported to a common graphic format (JPEG) and the proposed RNA folding structure can be downloaded in the Vienna format (Figure 3E). For both the secondary structures, the minimum free energy is calculated using the RNAfold program, when possible. SIREs prediction structures that fail to be folded by RNAfold program will show a minimum free energy of 0.0. A list of IRE features is displayed next to the graphs in the report section together with a small quality icon (green or yellow tick or red cross; Figure 3B and C). Each of these features displays interactive help information in widgets after being clicked. Benchmarking queries

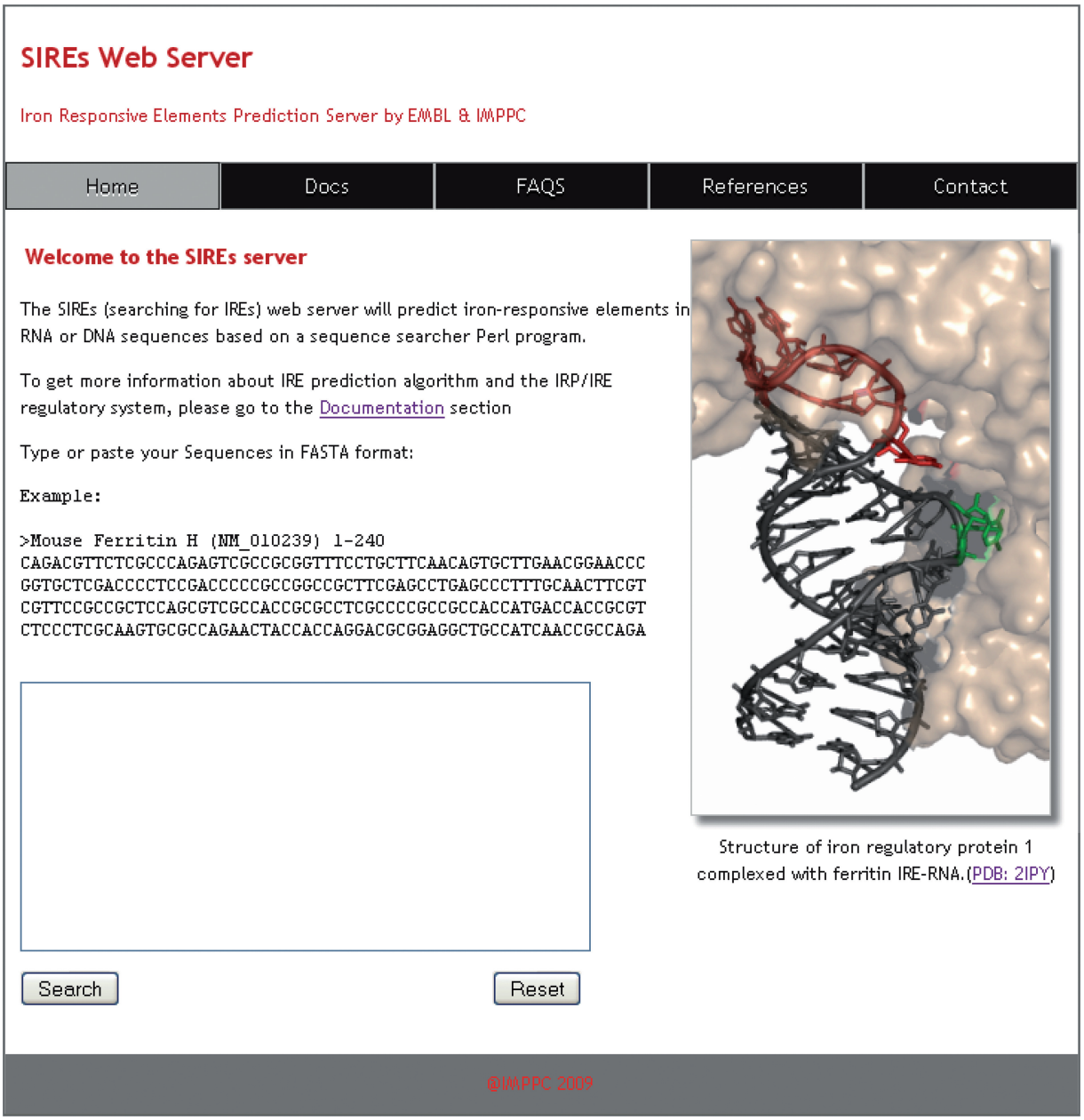

Figure 2. Input page of the SIREs web server. The input page of the SIREs web server provides a simplified form where only the sequence in FASTA format is required. A partial sequence of the 5′UTR of the mouse ferritin-H cDNA (GenBank Accession number: NM_010239, nucleotides 1–240) that contains an IRE is given as an example of the FASTA format that can also be used as a rapid testing example. A navigation area is also presented, containing links to the documentation, FAQs, references and contact sections.

containing up to 1000 sequence and 300 000 residues will typically run in <15 s. All the files generated by the server including the FASTA input sequence, the GFF summary file, all the structure images for both SIREs and RNA fold predictions, and the Vienna and FASTA formatted files for the predicted IREs can also be download in a single compressed file.

Confidence of IRE predictions

We have set three levels of stringency for assessing the confidence of the IRE predictions by the SIREs program. Reported features are scored and IREs are classified into three categories of confidence according to the sum score value: high (scores from 8 to 6); medium (scores from 5.9 to 4) and low (scores from 3.9 to 0). High confidence IRE predictions include all known and well characterized IREs *in vitro* and *in vivo* such as the IREs present in ferritin L, ferritin H, TFR1, ALAS2, ACO2, SLC40A1, dSDH, CDC14A, SLC11A2 and EPAS1. Medium and low confidence level predictions include IRE-like motifs that do not fulfill most of the IRE prediction criteria. SIREs program scores with a medium confidence flag the IREs present in the mouse Hao1 and the

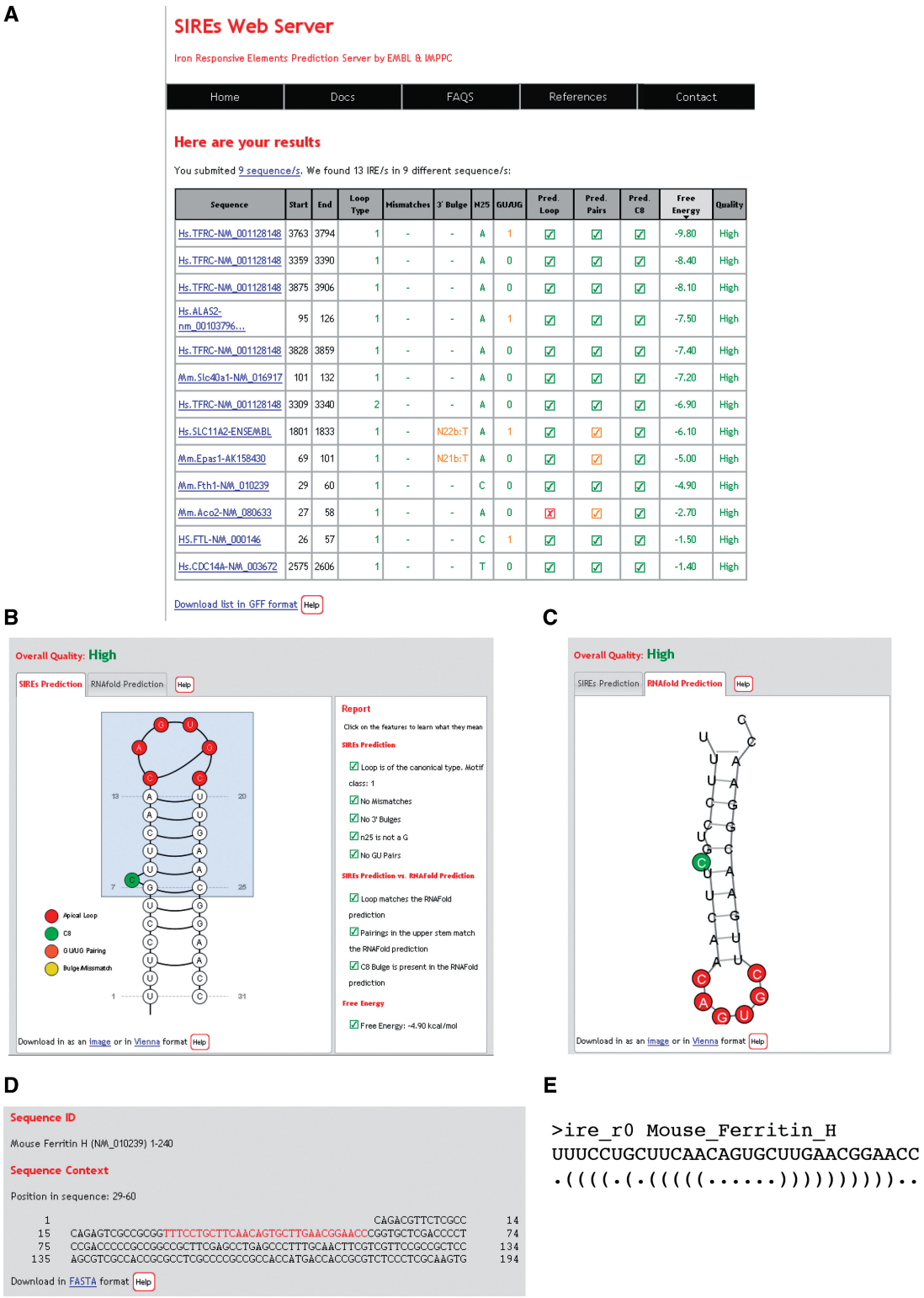

Figure 3. The SIREs web server output. (**A**) The top part shows navigation links to all different sections of the web site. Below, a summary of the results is shown, including the total number of submitted sequences and predicted IREs, and a detailed table with features of each predicted IRE. This table can be sorted by several criteria and its content can be downloaded in GFF standard format. Each row is linked to a more detailed report. (**B**) For each predicted IRE, a detailed report is presented including the overall quality of the prediction, a graphical representation of the predicted structure and detailed description of the predicted IRE features. The scheme includes a legend and highlights important IRE features, including the apical loop (in red), the C-8 bulge (in green), GU/UG base pairs (in orange) and other bulges or mismatches (in yellow). This image can be downloaded in JPEG format. To the right, a summary of the predicted IRE features is provided. By clicking in each feature, the user accesses a short description of it. (**C**) The user can switch from the scheme described before to a graphical representation of the RNA folded by the RNAfold program from the Vienna Package, where also the apical loop (in red) and the C8 bulge (in green) are highlighted. (**D**) For each predicted IRE, the sequence ID and sequence context is also provided, with the predicted IRE sequence shown in red. The IRE sequence can be downloaded in FASTA format by clicking on the provided link. (**E**) The SIREs web server also provides the conventional representation of the RNA folding in Vienna format.

human CDC42BPA mRNAs; evidence of *in vivo* functionality for these IREs has not yet been reported. IREs containing a SELEX apical motif (motifs 3 to 18) are penalized in the SIREs scoring system; thus, they are less probable to be reported as high quality predictions. To validate the predicted IREs reported by our program, we strongly recommend studying the *in vitro* functionality of the predicted IRE by competitive EMSA experiments (11,14) complemented by suitable functional tests *in vivo,* prioritizing high confidence IREs.

To evaluate the SIREs program, we use a data set of 35 novel IRP target genes recently identified and enriched on IRE-containing mRNAs (P = 6e-13, Fisher's exact test; Sanchez *et al*., manuscript in preparation) together with 150 random sequences that are not expected to harbor IRE elements. The random sequences were generated by random shuffling the nucleotides of 150 mouse RNA sequences arbitrarily selected. Novel IRP1 and IRP2 associated mRNAs were isolated by immunoprecipitation from five mouse tissues and detected by genome-wide microarray analysis. We identified 43 mRNAs able to bind both IRPs in at least one of the tested tissues, including all eight known murine IRE-containing mRNAs (Ftl, Fth1, Tfrc, Aco2, Alas2, Slc40a1, Slc11a2 and Epas1) and 35 previously unknown IRP target genes (Sanchez *et al*., manuscript in preparation).

Twenty-nine IREs were predicted by SIREs in 24 out of 35 novel IRP target genes. Figure 4 shows that canonical motifs 1 and 2 together with SELEX motif 8 constitute >65% of the total IREs detected by SIREs in this benchmark set of genes (27.6%, 24.1% and 13.8%, respectively).

Sensitivity, specificity and precision of the SIREs and three alternative IRE prediction programs (RNAAnalyzer, UTRScan and RNAMotif) were calculated and are reported in Table 1. Taking into consideration that not all IRP target genes may bind the IRPs through an IRE (29), it is likely that sensitivity values are underestimated. The data demonstrate the superior performance of the SIREs program compared with previously reported IRE search algorithms.

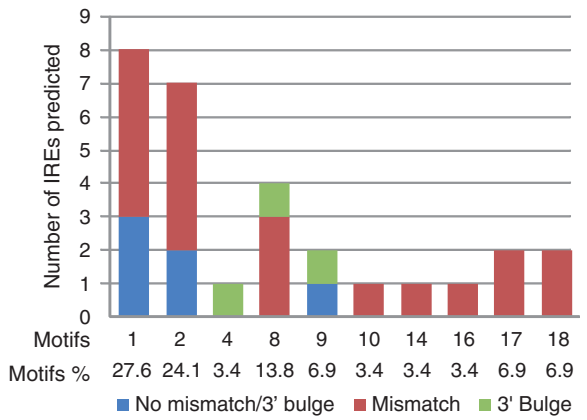

Figure 4. Motif distribution of the 35 IRP target genes used in SIREs evaluation. Twenty-nine IREs were predicted by SIREs in 24 out of 35 novel IRP target genes. Canonical motif 1 and 2 and SELEX motif 8 were detected more abundantly. Stem types inside each motif are classified by color as no mismatch/3′ bulge (blue), mismatch (red) or 3′ bulge (green).

DISCUSSION AND CONCLUSIONS

The SIREs web server is a bioinformatic tool to predict IRE-like motifs in nucleotide sequences. Existing software tools to predict this type of *cis*-regulatory element (RNAAnalyzer, UTRScan and RNAMotif) (24–26) are not sufficiently accurate to find atypical IREs due to their strict constraints for pattern matching searches. The major advantage of the SIREs program is that it is able to detect canonical and non-canonical IREs because it integrates and allows the combination of several experimentally reported IRE structures without losing stringency in its predictions. Therefore, with this program we can predict IRE motifs with 18 possible apical loop motifs, one single mismatch in the upper stem or one single 3′ bulge nucleotide and a maximum of two wobble base pairs. These extended combinations allow predicting all experimentally tested IREs not possible to be found until now with current bioinformatics tools and expand the IRE consensus secondary structure (21–23,27).

In addition, the SIREs program offers an overall quality flag for IRE prediction obtained by scoring the similarities between the predicted SIREs motif and the minimal energy conformational structure predicted by RNAfold program and the presence/absence of the abovementioned IRE structure characteristics.

IREs with medium or low flag quality have a lower confidence of prediction. The SIREs algorithm detects additional IREs in known IRE-containing mRNAs, such as in the human sequences of FTH1 (NM_002032), EPAS1 (NM_001430), ACO2 (NM_001098), SLC40A1 (NM_014585) and in the mouse sequence of SLC11A2 (AF029758). Any of these novel IREs have high confidence scores, and some of them even fail to be folded;

Table 1. Sensitivity, specificity and precision levels for SIREs and three additional IRE predicted softwares

	SIRES[a]			RNA Analyzer[b]	UTR Scan[c]	RNA Motif[d]
	Confidence level					
	Low	Medium	High			
Sensitivity (%)	69.6	51.4	25.7	14.2	11.4	2.85
Specificity (%)	91.3	95.3	99.3	99.3	99.3	99.3
Precision (%)	64.9	72.0	90.0	83.3	80.0	50.0

Sensitivity is the fraction of IRP target genes with at least one predicted IRE in a given stringent level in the set of the 35 novel IRP target genes. Specificity is the fraction of random sequences with at least one predicted IRE in a given stringent level in the set of 150 random sequences. Precision is the fraction of IRP target genes identified with at least one predicted IRE for a given stringent level in the set of 35 novel IRP target genes and 150 random sequences. For SIREs program we provide sensitivity, specificity and precision values for the three confidence level that the program provides.
[a]http://ccbg.imppc.org/sires/index.html.
[b]http://rnaanalyzer.bioapps.biozentrum.uni-wuerzburg.de/server.html.
[c]http://utrdb.ba.itb.cnr.it/tool/utrscan.
[d]http://casegroup.rutgers.edu/.
SIREs, searching for IREs.

suggesting that they are false positives. In fact, we could not functionally validate *in vitro* the highest scored of those IREs corresponding to a 3′IRE in ACO2 mRNA (motif 17 and medium level of confidence) by competitive EMSAs (data not shown).

In summary, the SIREs web server represents a significant improvement over currently available programs to predict IREs, providing the scientific community with an easy-to-use bioinformatics platform to identify putative IRE motifs that can then be subjected to further experimental testing *in vitro* and *in vivo*.

ACKNOWLEDGEMENTS

We thank Ana Rojas for helping with the beta-testing of the SIREs program and members of the BioIron community for testing the SIREs web server. We thank Yevhen Vainshtein for initial support in the development of the SIREs algorithm and Bruno Galy for helpful suggestions on the article.

FUNDING

'Instituto de Salud Carlos III', Spanish Health Program (Ministry of Science and Innovation; PS09/00341 to M.S.); Spanish Ministry of Science and Innovation (RYC-2008-02352 research contract under the Ramón y Cajal program to M.S.). Funding for open access charge: Institute of Predictive and Personalized Medicine of Cancer (IMPPC) in part.

Conflict of interest statement. None declared.

REFERENCES

1. Mata,J., Marguerat,S. and Bahler,J. (2005) Post-transcriptional control of gene expression: a genome-wide perspective. *Trends Biochem Sci.*, **30**, 506–514.
2. Muckenthaler,M.U., Galy,B. and Hentze,M.W. (2008) Systemic iron homeostasis and the iron-responsive element/iron-regulatory protein (IRE/IRP) regulatory network. *Annu. Rev. Nutr.*, **28**, 197–213.
3. Muckenthaler,M., Gray,N.K. and Hentze,M.W. (1998) IRP-1 binding to ferritin mRNA prevents the recruitment of the small ribosomal subunit by the cap-binding complex eIF4F. *Mol. Cell*, **2**, 383–388.
4. Binder,R., Horowitz,J.A., Basilion,J.P., Koeller,D.M., Klausner,R.D. and Harford,J.B. (1994) Evidence that the pathway of transferrin receptor mRNA degradation involves an endonucleolytic cleavage within the 3′ UTR and does not involve poly(A) tail shortening. *EMBO J.*, **13**, 1969–1980.
5. Smith,S.R., Ghosh,M.C., Ollivierre-Wilson,H., Hang Tong,W. and Rouault,T.A. (2006) Complete loss of iron regulatory proteins 1 and 2 prevents viability of murine zygotes beyond the blastocyst stage of embryonic development. *Blood Cells Mol. Dis.*, **36**, 283–287.
6. Galy,B., Ferring-Appel,D., Kaden,S., Grone,H.J. and Hentze,M.W. (2008) Iron regulatory proteins are essential for intestinal function and control key iron absorption molecules in the duodenum. *Cell Metab.*, **7**, 79–85.
7. Hentze,M.W., Rouault,T.A., Caughman,S.W., Dancis,A., Harford,J.B. and Klausner,R.D. (1987) A cis-acting element is necessary and sufficient for translational regulation of human ferritin expression in response to iron. *Proc. Natl Acad. Sci. USA*, **84**, 6730–6734.
8. Dandekar,T., Stripecke,R., Gray,N.K., Goossen,B., Constable,A., Johansson,H.E. and Hentze,M.W. (1991) Identification of a novel iron-responsive element in murine and human erythroid delta-aminolevulinic acid synthase mRNA. *EMBO J.*, **10**, 1903–1909.
9. McKie,A.T., Marciani,P., Rolfs,A., Brennan,K., Wehr,K., Barrow,D., Miret,S., Bomford,A., Peters,T.J., Farzaneh,F. *et al.* (2000) A novel duodenal iron-regulated transporter, IREG1, implicated in the basolateral transfer of iron to the circulation. *Mol. Cell*, **5**, 299–309.
10. Gray,N.K., Pantopoulos,K., Dandekar,T., Ackrell,B.A. and Hentze,M.W. (1996) Translational regulation of mammalian and Drosophila citric acid cycle enzymes via iron-responsive elements. *Proc. Natl Acad. Sci. USA*, **93**, 4925–4930.
11. Sanchez,M., Galy,B., Muckenthaler,M.U. and Hentze,M.W. (2007) Iron-regulatory proteins limit hypoxia-inducible factor-2alpha expression in iron deficiency. *Nat. Struct. Mol. Biol.*, **14**, 420–426.
12. Koeller,D.M., Casey,J.L., Hentze,M.W., Gerhardt,E.M., Chan,L.N., Klausner,R.D. and Harford,J.B. (1989) A cytosolic protein binds to structural elements within the iron regulatory region of the transferrin receptor mRNA. *Proc. Natl Acad. Sci. USA*, **86**, 3574–3578.
13. Gunshin,H., Mackenzie,B., Berger,U.V., Gunshin,Y., Romero,M.F., Boron,W.F., Nussberger,S., Gollan,J.L. and Hediger,M.A. (1997) Cloning and characterization of a mammalian proton-coupled metal-ion transporter. *Nature*, **388**, 482–488.
14. Sanchez,M., Galy,B., Dandekar,T., Bengert,P., Vainshtein,Y., Stolte,J., Muckenthaler,M.U. and Hentze,M.W. (2006) Iron regulation and the cell cycle: identification of an iron-responsive element in the 3′-untranslated region of human cell division cycle 14A mRNA by a refined microarray-based screening strategy. *J. Biol. Chem.*, **281**, 22865–22874.
15. Cmejla,R., Petrak,J. and Cmejlova,J. (2006) A novel iron responsive element in the 3′UTR of human MRCKalpha. *Biochem. Biophys. Res. Commun.*, **341**, 158–166.
16. Kohler,S.A., Menotti,E. and Kuhn,L.C. (1999) Molecular cloning of mouse glycolate oxidase. High evolutionary conservation and presence of an iron-responsive element-like sequence in the mRNA. *J. Biol. Chem.*, **274**, 2401–2407.
17. Beaumont,C., Leneuve,P., Devaux,I., Scoazec,J.Y., Berthier,M., Loiseau,M.N., Grandchamp,B. and Bonneau,D. (1995) Mutation in the iron responsive element of the L ferritin mRNA in a family with dominant hyperferritinaemia and cataract. *Nat. Genet.*, **11**, 444–446.
18. Kato,J., Fujikawa,K., Kanda,M., Fukuda,N., Sasaki,K., Takayama,T., Kobune,M., Takada,K., Takimoto,R., Hamada,H. *et al.* (2001) A mutation, in the iron-responsive element of H ferritin mRNA, causing autosomal dominant iron overload. *Am. J. Hum. Genet.*, **69**, 191–197.
19. Hentze,M.W., Caughman,S.W., Casey,J.L., Koeller,D.M., Rouault,T.A., Harford,J.B. and Klausner,R.D. (1988) A model for the structure and functions of iron-responsive elements. *Gene*, **72**, 201–208.
20. Theil,E.C. and Eisenstein,R.S. (2000) Combinatorial mRNA regulation: iron regulatory proteins and iso-iron-responsive elements (Iso-IREs). *J. Biol. Chem.*, **275**, 40659–40662.
21. Henderson,B.R., Menotti,E., Bonnard,C. and Kuhn,L.C. (1994) Optimal sequence and structure of iron-responsive elements. Selection of RNA stem-loops with high affinity for iron regulatory factor. *J. Biol. Chem.*, **269**, 17481–17489.
22. Henderson,B.R., Menotti,E. and Kuhn,L.C. (1996) Iron regulatory proteins 1 and 2 bind distinct sets of RNA target sequences. *J. Biol. Chem.*, **271**, 4900–4908.
23. Butt,J., Kim,H.Y., Basilion,J.P., Cohen,S., Iwai,K., Philpott,C.C., Altschul,S., Klausner,R.D. and Rouault,T.A. (1996) Differences in the RNA binding sites of iron regulatory proteins and potential target diversity. *Proc. Natl Acad. Sci. USA*, **93**, 4345–4349.
24. Macke,T.J., Ecker,D.J., Gutell,R.R., Gautheret,D., Case,D.A. and Sampath,R. (2001) RNAMotif, an RNA secondary structure definition and search algorithm. *Nucleic Acids Res.*, **29**, 4724–4735.

25. Bengert,P. and Dandekar,T. (2003) A software tool-box for analysis of regulatory RNA elements. *Nucleic Acids Res.*, **31**, 3441–3445.
26. Mignone,F., Grillo,G., Licciulli,F., Iacono,M., Liuni,S., Kersey,P.J., Duarte,J., Saccone,C. and Pesole,G. (2005) UTRdb and UTRsite: a collection of sequences and regulatory motifs of the untranslated regions of eukaryotic mRNAs. *Nucleic Acids Res.*, **33**, D141–D146.
27. Goforth,J.B., Anderson,S.A., Nizzi,C.P. and Eisenstein,R.S. (2010) Multiple determinants within iron-responsive elements dictate iron regulatory protein binding and regulatory hierarchy. *RNA*, **16**, 154–169.
28. Gruber,A.R., Lorenz,R., Bernhart,S.H., Neubock,R. and Hofacker,I.L. (2008) The Vienna RNA websuite. *Nucleic Acids Res.*, **36**, W70–W74.
29. Rogers,J.T., Randall,J.D., Cahill,C.M., Eder,P.S., Huang,X., Gunshin,H., Leiter,L., McPhee,J., Sarang,S.S., Utsuki,T. *et al.* (2002) An iron-responsive element type II in the 5′-untranslated region of the Alzheimer's amyloid precursor protein transcript. *J. Biol. Chem.*, **277**, 45518–45528.